

Pressure-dependent resistivity and magnetoresistivity of erbium

Mark Ellerby and Keith A. McEwen

Department of Physics and Astronomy, University College London, Gower Street, London WC1E 6BT, England

Ernst Bauer and Robert Hauser

Institut für Experimentalphysik, Technische Universität Wien, A-1040 Wien, Austria

Jens Jensen

Ørsted Laboratory, Niels Bohr Institute fAPG, Universitetsparken 5, 2100 Copenhagen, Denmark

(Received 6 August 1999)

A comprehensive resistance study of erbium subjected to a hydrostatic pressure is presented. From the experimental results we derive a p - T phase diagram for the magnetic phases in erbium. In the zero-temperature limit, the conical structure is predicted to transform into the cycloidal one at a pressure of about 1.3 kbar. Experimentally, the transition is found to occur between 1 and 3 kbar at 4.5 K. The experimental results are analyzed in terms of a variational calculation of the resistivity using the model developed for erbium from previous experiments. The theory of Elliott and Wedgwood is utilized in the account of the superzone effects. The analysis indicates that the a -axis resistivity is slightly affected by the superzones. In the c -axis case the superzone effects do not simply scale with the magnetization, but also reflect the 20% change of the ordering wave vector. This occurs between T_N and T_C at ambient pressure, and at 4.5 K when the pressure is increased from 1 to 3 kbar. It is tentatively proposed that the tilted cycloidal structure exists in Er, just above T_C at ambient pressure and in the interval between 1.3 and 9 kbar at zero temperature.

I. INTRODUCTION

The first detailed neutron-diffraction study of erbium was reported by Cable *et al.*¹ They found that between $T_N = 84$ K and 52 K the magnetic structure is c -axis modulated (CAM) with the amplitude of the moments varying sinusoidally. The ordering wave-vector \mathbf{Q} is close to $\frac{2}{7} \mathbf{c}^*$. Below $T'_N = 52$ K the moments in the basal plane are ordered, and \mathbf{Q} gradually decreases to become $\frac{1}{4} \mathbf{c}^*$ just above $T_C = 18$ K. For temperatures below T_C they observed a conical structure with the moments parallel to the c axis being ferromagnetic and the moments in the basal plane forming a helix. These early results were confirmed by Habenschuss *et al.*,² who observed a gradual development of higher harmonics with decreasing temperatures indicating that the structure is squaring up. Gibbs *et al.* found a series of lock-in phases below T'_N using magnetic x-ray scattering.³ These commensurate structures are regular arrangements of 3 or 4 hexagonal layers of moments with an alternating positive or negative component along the c axis. The seven-layered (43)-structure observed close to T'_N thus comprises 4 hexagonal planes of moments with a positive c -component followed by 3 planes of moments with a negative c -component. As the temperature is lowered, triplets are progressively replaced by quartets, until the system just above T_C consists of quartets only, which is the (44)-structure with $q = \frac{1}{4} \mathbf{c}^*$. Using a large single crystal and a triple-axis spectrometer for isolating the purely elastic scattered neutrons, Cowley and Jensen were able to determine the intensities of most of the harmonics in the commensurate structures of Er.^{4,5} The experimental results were compared with the diffraction intensities of the corresponding structures predicted by a mean-field model. This comparison confirmed that the basic feature of the commensurate structures is the one proposed by Gibbs *et al.* The neutron experiments also showed the presence of scattering

peaks along the c axis at $\pm(2n+1)Q + mc^*$ for odd integer values of m . These indicate that the magnetic structures depend on the two orientations of the hexagonal layers in the hcp lattice, implying that the structures are distorted by interactions which have threefold symmetry around the c axis. The resulting structures between T_C and T'_N are “wobbling cycloids,” in which there is a small b -axis moment oscillating with a period different from that of the basic cycloidal structure lying in the a - c plane. Because of this b -axis component, the (43)-structure should rather be denoted the 2(43)-structure, as it only repeats itself after each 14 layers. The “trigonal” couplings in Er produce a nonplanar distortion of the cycloidal structure and probably also cause the lock-in effect at $\mathbf{Q} = \frac{5}{21} \mathbf{c}^*$ observed in the cone phase (the cone angle in Er is so small, about 28°, that the hexagonal anisotropy is unimportant).

There has been considerable activity in the study of erbium with a focus on the magnetic phase diagrams. Notable amongst these are the neutron-diffraction studies of Er in a c -axis field by Lin *et al.*⁶ and by McMorro *et al.*⁷ The general features of the two phase diagrams are quite similar, with some differences in the cycloidal phase. The magnetic phase diagram has also been derived by Eccleston and Palmer⁸ from ultrasonic attenuation and by Zochowski and McEwen⁹ from thermal expansion and magnetostriction studies. Both results show correspondence with the diagrams determined from the neutron-diffraction studies. The magnetic phase diagram for a field applied in the basal plane has been derived from neutron diffraction by Jehan *et al.*¹⁰ and from resistivity measurements by Watson and Ali.¹²

The thermal-expansion measurements performed on Er by Rhyne and Legvold¹¹ revealed abrupt changes of the α -strain parameters, ϵ_{33} and $\epsilon_{11} + \epsilon_{22}$, at T_C . Utilizing this result, Jensen and Mackintosh predicted that the magnetoelastic en-

ergies would cause the cone structure to be unstable at all temperatures, when applying a hydrostatic pressure of more than approximately 2.5 kbar.¹³ There have been two recent reports of the influence of hydrostatic pressure on the magnetic structures of Er by Kawano *et al.*^{14,15} They measured the magnetic Bragg peaks at an applied pressure of 11.5 and 14 kbar. At 11.5 kbar T_N is reduced to 82 K. The ordering wave vector goes through a maximum at 50 K, and below about 40 K it stays constant at the value $\frac{2}{7} c^*$. From their analysis they concluded that the structure is cycloidal below $T'_N \approx 46$ K down to the lowest temperature studied (4.5 K). There have been several early studies of bulk and transport properties for Er under hydrostatic pressure.^{16–18} However, to date, there exists no detailed exposition of the p - T phase diagram for erbium.

In this paper we present the results of resistivity measurements made on a single crystal of erbium. The measurements were made on a longitudinal c -axis sample under hydrostatic pressure. From these measurements we derive a p - T phase diagram. In accordance with previous experiments at ambient pressure,¹⁹ the c -axis resistivity shows a rapid increase below T_N . This is ascribed to the development of gaps in the electronic bands at the superzone boundaries introduced by the magnetic periodicity.²⁰ The theory was developed by Miwa for the particular case of Er,²¹ and a more general account was later presented by Elliott and Wedgwood.^{22,23} Here, the magnetoresistance of Er is analyzed using the same theoretical approach applied recently in the case of thulium.²⁴ The variational result for the resistivity is combined with the Elliott-Wedgwood theory for the superzone effects, and the magnetic response function is determined from the RPA model^{4,5} derived for Er from previous neutron-scattering experiments.

II. EXPERIMENTAL DETAILS

A large single crystal of erbium was grown using the strain-anneal method described in Ref. 25 and was cut from the same ingot as the crystal used in Ref. 9. The dimensions of the c -axis resistivity sample were $A_r = 5.5 \times 10^{-3}$ cm² (cross-sectional area) and $l = 0.45$ cm (separation between voltage probes).

The pressure-dependent resistance measurements were made, in Vienna, with the current parallel to the c axis using a 4-terminal dc method. The voltage was measured with a Keithley-181 nanovoltmeter and a constant current of 30 mA was provided by a Knick constant current power-supply. The cryostat was a Cryophysics variable temperature insert (VTI) with a temperature range between 1.5 and 300 K. The temperature was controlled and measured using calibrated germanium and platinum resistance thermometers in conjunction with a Lakeshore DRC-91C Controller. The hydrostatic pressure was applied using a clamp cell with a teflon capsule. The pressure transmitting medium was a mixture of 4:1 ethanol-methanol. The pressure was determined using two manometers. The purpose of the two manometers was to ensure that the pressure remained stable across the entire temperature range. All the measurements were made by heating the sample at constant pressure.

The magnetoresistance measurements reported here were performed in London also using a 4-terminal dc method. The

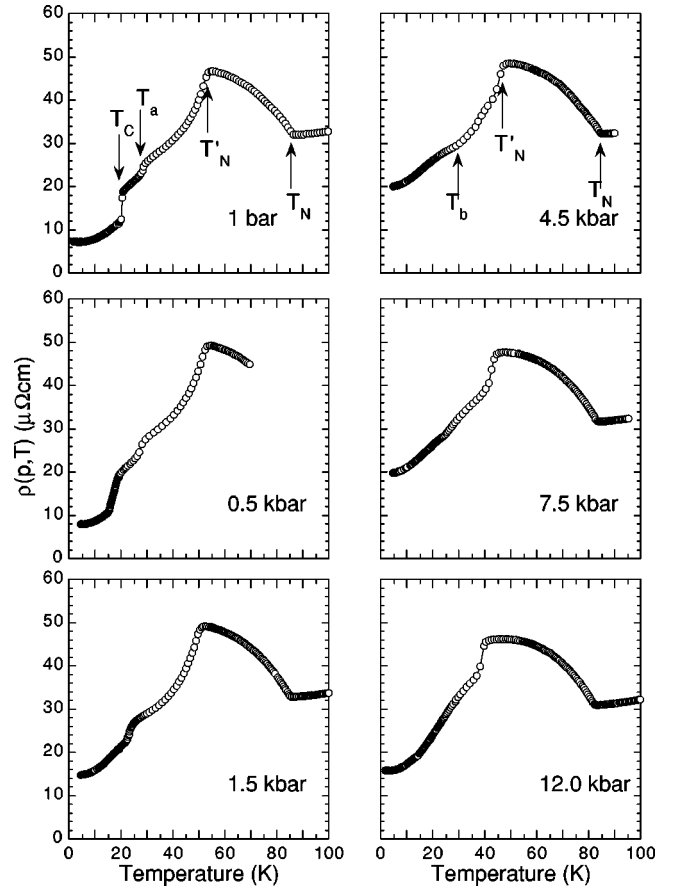


FIG. 1. The isobaric temperature dependence of the c -axis resistivity, with the temperatures of the various transitions and anomalies indicated by arrows.

voltage was measured with a Keithley-181 nanovoltmeter and a constant current of 30 mA was provided by a Keithley-220 constant current power-supply. The cryostat was an Oxford variable-temperature insert (VTI) with a temperature range between 1.6 and 300 K. This cryostat was mounted in a vertical-field magnet which could achieve fields of up to 7 T. The temperature was controlled and measured using a calibrated carbon-glass thermometer in conjunction with a Lakeshore DRC-93C Controller. Two geometries were studied in the magnetoresistance. The first series of measurements were made with the current and field parallel to the c axis (longitudinal), and the second set of measurements were made with the current parallel to the c axis and the field parallel to the a axis (transverse). Both sets of measurements were made while cooling the sample in constant field.

III. EXPERIMENTAL RESULTS AND p - T PHASE DIAGRAM

Figure 1 shows measurements of the temperature dependence of the c -axis resistivity at a series of constant hydrostatic pressures. The figures have been annotated with arrows to indicate the various observed transitions or anomalies. The measurement at 1 bar is consistent with earlier measurements.¹⁹ The resistivity increases below $T_N = 85$ K until the temperature derivative changes its sign at $T'_N = 52$ K. In the cycloidal phase below this temperature there is an

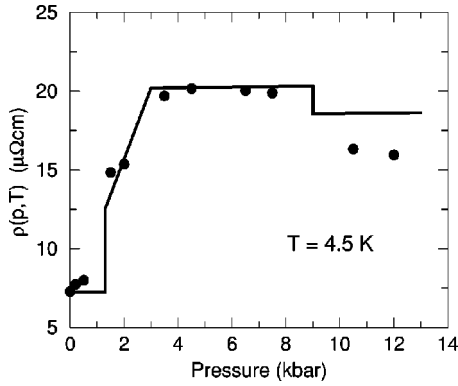


FIG. 2. The isothermal pressure dependence of the c -axis resistivity in Er at 4.5 K. The theoretical result shown by the solid line is discussed in Sec. V.

anomaly at $T_a=27.5$ K and the resistivity finally decreases rapidly at $T_C=20.2$ K. The application of a hydrostatic pressure of $p=0.5$ kbar introduces slight shifts in the positions of the anomalies. However, there is a significant change in the transition at T_C , which becomes much broader with the midpoint shifted to $T_C=17.3$ K. At higher values of the pressure, $p \geq 1.5$ kbar, the transition between the cycloid and the cone structures is no longer discernible from the data. However, at 1.5 kbar there is still an anomaly in the temperature derivative located at 11 K. At $p=4.5$ kbar the anomaly at T_a is too weak to be identified. Instead a new one has appeared at T_b , which becomes more pronounced at 7.5 kbar, and is still visible in the derivative of the resistivity at 12 kbar.

The ferromagnetic cone structure is difficult to track in the temperature-dependent measurements and therefore we present an isothermal plot of the pressure dependence of the resistivity at $T=4.5$ K in Fig. 2. Between $p=0.5$ and 3.5 kbar there is a rapid increase in the resistivity. It stays nearly constant between 3.5 and 7.5 kbar and is then observed to decrease to a new constant level existing above 10.5 kbar. As discussed in more detail in the next section, the measurements show that the superzone effects in Er not only depend on the size of the energy gaps but also on their positions in reciprocal space. Therefore, one possible explanation of the isothermal behavior shown in Fig. 2 is that the transition from the cone to the cycloidal phase occurs in the interval from 0.5 to 1.5 kbar, which, in the next interval between 2.0 and 3.5 kbar, is followed by a large change of the ordering wave vector \mathbf{Q} from about $\frac{1}{4} \mathbf{c}^*$ to about $\frac{2}{7} \mathbf{c}^*$. It is clear from the isobaric behavior that the application of the hydrostatic pressure broadens the first-order transition between the cycloidal structure and the cone. The c/a -ratio changes by about 0.5% at the transition which may give rise to an inhomogeneous distribution of domains when p is close to the critical pressure. The present experiments indicate that the transition from the cone to the cycloidal structure at 4.5 K is accomplished fully, at least at the pressure of 3.5 kbar, and thus that the critical pressure has a value lying between 1 and 3 kbar. A more precise description of the transition will require a direct determination of the structures by diffraction measurements.

Figures 1 and 2 show a selection of the data gathered in the pressure experiments. The total number of results have been used to construct the p - T phase diagram for erbium

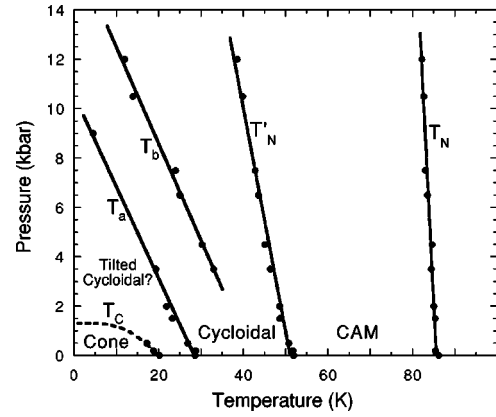


FIG. 3. p - T phase diagram for erbium. The solid lines are linear fits to the data with the fit parameters listed in Table I. The dashed line shows the theoretical estimate of T_C .

which is presented in Fig. 3. With the exception of T_N all the transition temperatures in the diagram show hysteresis. The results shown here were obtained on heating, and the anomalies below T_N are shifted down by 2–4 K on cooling. The phase diagram may be compared with previous results obtained by Milton and Scott,¹⁶ who measured the ac-inductance of polycrystalline Er as a function of temperature at various pressures ranging from 0 to 7 kbar. As shown in Table I our results for the pressure dependence of T_N and T'_N are in reasonable agreement with those of Ref. 16. In the measurements of Milton and Scott the anomaly observed at T_C is weak and disappears with pressure above 3 kbar. Their result for dT_C/dp is a factor of 7 smaller than ours, but both results depend on the way the measurements are interpreted and are subjected to large uncertainties. Milton and Scott also reported a transition centered at $T \approx 27$ K. This observation appears to agree with the anomaly marked by T_a in the present study. However, the influence of pressure differs in the two cases, as the position of the peak observed by Milton and Scott was nearly unchanged when the pressure was varied.

As discussed in Ref. 13 the low-temperature cone structure is destabilized by a hydrostatic pressure due to two-ion magnetoelastic interactions. Defining $\Delta \epsilon_{\alpha\alpha} = \epsilon_{\alpha\alpha}(\text{cone}) - \epsilon_{\alpha\alpha}(\text{cycloid})$ then the thermal-expansion measurements indicate that $\Delta \epsilon_{33} = 3.1 \times 10^{-3}$ and $\Delta(\epsilon_{11} + \epsilon_{22}) = -2.4 \times 10^{-3}$ at T_C (at ambient pressure).¹¹ These values were used in the comparison of the elastic energy difference with the magnetic free-energy difference between the two structures calculated from the mean-field model of Er.¹³ In the

TABLE I. Parameters deduced from linear fit to data in p - T phase diagram, compared with the results (Ref. 16) of Milton and Scott shown in the last column.

	Temperature (K)	dT/dp (K/kbar)	dT/dp (K/kbar) (Ref. 16)
T_N	85.8 ± 0.1	-0.31 ± 0.02	-0.26 ± 0.2
T'_N	51.0 ± 0.3	-1.09 ± 0.05	-1.3 ± 0.2
T_b	42 ± 1	-2.54 ± 0.13	
T_a	28.3 ± 0.4	-2.66 ± 0.11	
T_C	20.5 ± 0.3	-6.0	-0.8

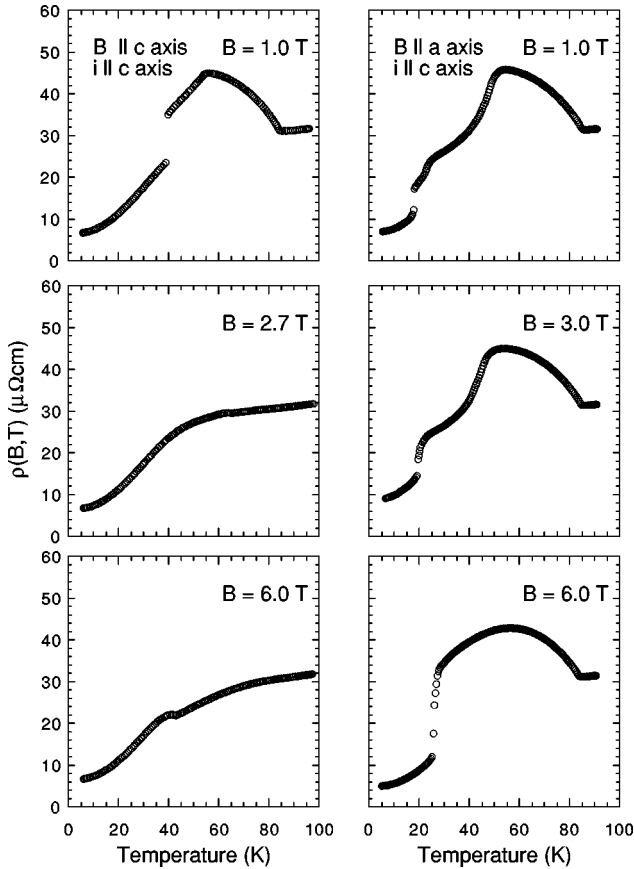


FIG. 4. Magnetoresistance along the c axis of Er in a field applied parallel to the c axis (left) and parallel to the a axis (right).

zero-temperature limit the magnetic energy difference was estimated to be 0.033 meV/ion corresponding to a critical hydrostatic pressure of 2.5 kbar. The present mean-field model of Er leads to the higher value of 0.051 meV/ion for this energy difference. On the other hand the neutron-diffraction experiments of Habenschuss *et al.* show changes of the lattice parameters at the transition,² which are $\Delta \epsilon_{33} = 3.9 \times 10^{-3}$ and $\Delta(\epsilon_{11} + \epsilon_{22}) = -2.0 \times 10^{-3}$. Using their results and the average value for the calculated energy difference between the two structures, the critical pressure at zero temperature is derived to be 1.3 ± 0.3 kbar (the absolute lower limit is about 0.9 kbar and the upper one 3.8 kbar). The calculated phase-line corresponding to this estimate is included as a dashed line in Fig. 3.

In Fig. 4 we present the results of a magnetoresistance study for Er with the current parallel to the c axis. The left side of the figure shows the longitudinal resistivity and on the right we present the transverse resistivity with \mathbf{B} parallel to the a axis. The longitudinal magnetoresistivity shows that at $B = 1.0$ T the Néel transition is at $T_N = 84.3$ K and is followed by a transition at $T'_N = 54$ K. Below this temperature the resistivity decreases almost linearly until at $T_C = 37$ K there is a sharp decrease in the resistivity. For a constant field $B = 2.7$ T the temperature dependence of the resistivity has changed dramatically. There is a small increase at $T = 65$ K and the position of this feature was found to decrease in temperature as the field was increased. For $B = 6.0$ T this transition is more pronounced and occurs at $T = 43$ K. We attribute this anomaly to the transition between the paramag-

netic and the conical phase.^{6,7} The c -axis field suppresses the modulated ordering of the c -axis moments, so that the only possible structures left for $B \geq 2.7$ T are the paramagnet and the cone. The superzone effects are relatively small in the cone phase. In contrast, a field applied along the a axis has little effect on the modulated ordering of the moments along the c axis. Thus in this configuration, the effects of the superzones are large, even at a field of 6 T, until the c -axis moments become ferromagnetically aligned at low temperatures. The structures produced at intermediate values of the a -axis field are complicated fan structures which have been studied by Jehan *et al.*¹⁰

IV. THEORETICAL ANALYSIS OF THE RESISTANCE MEASUREMENTS

The experimental results show a number of dramatic effects of the magnetic ordering of Er on the resistivity. The most important coupling between the conduction electrons and the magnetic moments of the $4f$ electrons is the Ruderman-Kittel-Kasuya-Yosida (RKKY)-exchange interaction. The effects of this coupling on the resistivity have been discussed in detail in a previous paper analyzing the magnetoresistance of thulium.²⁴ Assuming a free-electron-like behavior of the conduction electrons and neglecting the \mathbf{q} dependence of the RKKY coupling, the uu -component of the magnetic resistivity, defined by the unit vector $\hat{\mathbf{u}}$, may be written^{13,24,26}

$$\rho_{\text{mag}}^{uu} = \frac{\rho_{\text{spd}}}{J(J+1)} \int_{-\infty}^{\infty} d(\hbar\omega) \frac{\hbar\omega/k_B T}{4 \sinh^2(\hbar\omega/2k_B T)} \times \sum_{\alpha} \frac{1}{\pi} \langle \chi''_{\alpha\alpha}(\mathbf{q}, \omega) \rangle_{\mathbf{q}}, \quad (1)$$

where the weighted \mathbf{q} average of the susceptibility tensor components is given by

$$\langle \chi''_{\alpha\alpha}(\mathbf{q}, \omega) \rangle_{\mathbf{q}} = \frac{12}{(2k_F)^4} \int_0^{2k_F} q dq \int \frac{d\Omega_{\mathbf{q}}}{4\pi} (\mathbf{q} \cdot \hat{\mathbf{u}})^2 \chi''_{\alpha\alpha}(\mathbf{q}, \omega) \quad (2)$$

[the factor 3 in Eq. (4.4) of Ref. 24 should be replaced by 12]. In the high-temperature limit the magnetic resistivity saturates at ρ_{spd} which is proportional to the square of the matrix element of the RKKY coupling. The total resistivity is the sum of three contributions,

$$\rho_0^{uu} = \rho_{\text{res}}^{uu} + \rho_{\text{phon}}^{uu} + \rho_{\text{mag}}^{uu}. \quad (3)$$

The impurity contribution ρ_{res}^{uu} is assumed to be independent of temperature and applied field or pressure. The phonon contribution is determined by the Bloch-Grüneisen formula

$$\rho_{\text{phon}}^{uu} = \rho_{\Theta}^{uu} \left(\frac{T}{\Theta} \right)^5 \int_0^{\Theta/T} \frac{z^5}{\sinh^2(z/2)} dz, \quad (4)$$

with the Debye temperature $\Theta = 192$ K for Er.

In the case of thulium, the absorptive part of the susceptibility tensor is quite well described by its mean-field value, averaged over the different sites,²⁴

$$\langle \chi''_{\alpha\alpha}(\mathbf{q}, \omega) \rangle_{\mathbf{q}} \approx \frac{1}{N} \sum_i \chi''_{\alpha\alpha}(i, \omega)|_{\text{MF}}. \quad (5)$$

We expect the same to be true in erbium, with the exception that the low-energy spin waves may be important in the cone phase in the low temperature limit. Close to a magnetic Bragg peak at \mathbf{Q} the dispersion of the spin waves¹³ is linear, $\varepsilon \approx A|\mathbf{q}-\mathbf{Q}|$, and to leading order in $k_B T$ we find

$$\langle \chi''_{\alpha\alpha}(\mathbf{q}, \omega) \rangle_{\mathbf{q}}^{\text{sw}} \approx \frac{\rho_{\text{spd}} L \sin^2 \theta_c (\pi k_B T)^2}{(J+1)A^3 (2k_F)^4} \sum_{\mathbf{K}=\tau \pm \mathbf{Q}}^{|K| < 2k_F} \frac{(\mathbf{K} \cdot \hat{\mathbf{u}})^2}{|\mathbf{K}|}, \quad (6)$$

where τ is a reciprocal-lattice vector. $L \sin^2 \theta_c \approx 5$ meV is an axial anisotropy parameter and $A \approx 12$ meV \AA .

The effective number of electrons carrying the current depends on the magnetic ordering via the RKKY interaction. The most significant changes occur when the $4f$ moments are oscillating. The RKKY coupling then leads to energy gaps at the superzone boundaries at $(\tau \pm n\mathbf{Q})/2$, where \mathbf{Q} is the magnetic ordering wave vector. The leading-order term corresponds to $n=1$, but the squaring up of the ordered moments and the higher-order coupling processes introduce values of n different from 1. The energy gaps are proportional to the harmonics of the oscillating moments and may be estimated to be of the order 0.1–0.2 eV in Er at maximum. Considering only the first harmonic of the moments, then in the free electron model, the four electronic modes at $\pm\mathbf{Q}/2$ are split by two gaps given by

$$\Delta_{\pm} = |\sqrt{\Delta_y^2 + \Delta_z^2} \pm \Delta_x|, \quad (7)$$

where Δ_{α} is a RKKY-coupling constant times the first harmonic of the α component of the ordered moments. It is assumed that both the x and y components, and the x and z components, are 90° out of phase. In the CAM-phase only Δ_z is nonzero and the average gap $\Delta = (\Delta_+ + \Delta_-)/2 = \Delta_z$. In the cycloidal phase both Δ_x and Δ_z are nonzero, and are, in general, different from each other corresponding to an ellipsoidal polarization. In the case of Er $\Delta_z > \Delta_x$ and the average gap is again $\Delta = \Delta_z$. In the cone phase $\Delta_z = 0$ and $\Delta_x = \Delta_y$ in which case $\Delta = \Delta_x$.

As discussed in detail by Elliott and Wedgwood²² the largest effects of the energy gaps occur when the superzone boundary touches or cuts through the Fermi surface. In this case the resistivity is divided by a factor which is linear in the corresponding averaged energy gap:

$$\rho^{uu} = \frac{\rho_0^{uu}}{1 - \delta_u}, \quad \delta_u = \Gamma_u \frac{\Delta}{\Delta_0}. \quad (8)$$

Introducing Γ_u as the effective value determined by the sum of all the contributions which are linear in the superzone gaps, then it is normally considered to be constant for the u th resistivity component. In the free-electron model only the c -axis resistivity is affected. In the case of the basal-plane resistivity, the condition $\hat{\mathbf{u}} \cdot \mathbf{Q} = 0$ ensures that the terms linear in Δ vanish, however, the coupling of the electrons with the lattice may in principle introduce such terms.

The resistivity of erbium in the different phases has been calculated from the equations above. The mean-field value of the susceptibility tensor in Eq. (5) was determined using the

TABLE II. Resistivity parameters in units of $\mu\Omega$ cm, and Γ_u^0 defined in Eq. (9) assuming M_1^0 to be the calculated maximum value of 10.9 μ_B .

Component	ρ_{res}	ρ_{Θ}	ρ_{spd}	Γ_u^0
cc	5.86	21.5	18.0	0.71
aa	8.4	50.0	32.4	0.14

model established by Cowley and Jensen,⁴ which includes the trigonal coupling. In spite of the better description of the magnetic properties of Er offered by the present model, and the use of the more accurate variational result for the resistivity, the calculated result for the cc -component at ambient pressure does not differ much from that obtained by Miwa.²¹ This means that the discrepancies between the calculated and the experimental results are rather large in the intermediate phase between T'_N and T_C , and, for instance, the jump predicted at T_C is about twice the observed one. The result for Er obtained by Elliott and Wedgwood²² compares even worse with the experimental resistivity. They assumed that the basal-plane components are ordered in a helix ($\Delta_x = \Delta_y$) between T'_N and T_C . This was also the structure considered by Cable *et al.*,¹ but as discussed by Cowley and Jensen, this structure may only occur under certain specialized conditions, and it is not compatible with the results of their diffraction experiments.⁴

The theory does not account satisfactorily for the temperature dependence of the resistivity in the cycloidal phase of Er at 1 bar. However, the comparison is much improved when considering the present results obtained at hydrostatic pressures exceeding 4.5 kbar. The only significant difference between the cycloidal structures at low and high values of the pressure is the way the ordering wave vector depends on temperature. The neutron diffraction experiments show that Q stays constant at $\frac{2}{7}c^*$ below T'_N at 11.5 and 14 kbar,¹⁵ in contrast to the rapid variation, by about 20%, shown by Q at ambient pressure. Hence, the only explanation for the deficiency of the theory at low pressure is that Γ_u in Eq. (8) does not stay constant but depends on Q . The dependence is assumed linear in Q and Eq. (8) is replaced by

$$\delta_u = \Gamma_u^0 \left[1 + \kappa \left(\tilde{Q} - \frac{2}{7} \right) \right] \frac{M_1}{M_1^0}, \quad \kappa = 6, \quad (9)$$

where \tilde{Q} is the length of the magnetic ordering vector in units of $2\pi/c$. The energy-gap ratio in Eq. (8) has been substituted by the ratio between the corresponding amplitudes of the first harmonic. κ is a fitting parameter determined to be 6. The calculated results, using this equation together with the resistivity fitting parameters given in Table II, are compared with the experiments at 1 bar and 7.5 kbar in Fig. 5. In the fit at ambient pressure we have used the temperature dependence of Q measured by Habenschuss *et al.* (on heating).² The experimental results at 6.5, 7.5, 10.5, and 12 kbar are nearly identical, except for the alterations due to the systematic shifts in the transition temperatures and the (minor) differences shown in Fig. 2, which appear below 10–20 K. This indicates that Q must behave in the same way in the four cases and similar to that measured by Kawano *et al.*¹⁵ at 11.5 and 14 kbar. Thus, at 7.5 kbar, Q

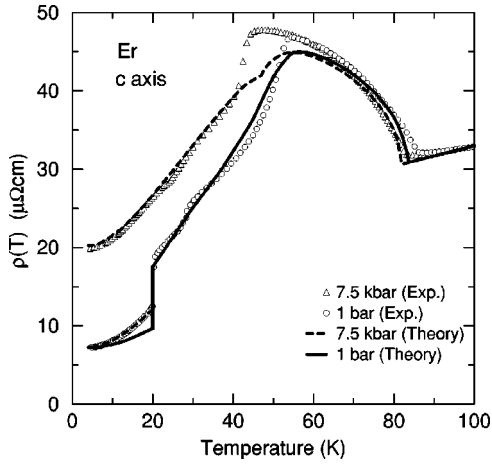


FIG. 5. Experimental and calculated temperature dependence of the c -axis resistivity of Er at 1 bar and 7.5 kbar.

is assumed to be locked to the value $\frac{2}{7} c^*$ below about 45 K, and to be the same as at ambient pressure above this temperature. The variation of T_N and T'_N with pressure shown in Fig. 3 is simulated in the calculations by scaling the exchange parameter $\mathcal{J}(\mathbf{Q})$ and the anisotropy parameter B_2^0 by the factors $(1 - 0.005 \tilde{p})$ and $(1 + 0.007 \tilde{p})$, respectively, where \tilde{p} is the pressure in units of kbar.

The difference between the results at 1 bar and 7.5 kbar in the intermediate phase, between T_C and T'_N , is explained almost exclusively by the Q -dependent factor in Eq. (9). The comparison in Fig. 5 between experiments and theory is satisfactory except for two major discrepancies. The one close to T'_N may be due to a slightly different temperature dependence of Q than the one assumed. The results of Atoji²⁷ show a more rapid variation of Q close to T'_N than used here. At 7.5 kbar Q may continue to increase below 55 K until a more abrupt reduction of Q sets in at T'_N . The experimental results of Kawano *et al.* at 14 kbar show some indications of this behavior.¹⁵ The other discrepancy concerns the low-temperature variation of the resistivity in the cone phase at ambient pressure. The experimental variation is quite well described by a T^2 dependence and might be due to the low-energy spin waves in this phase. The dotted line through the experimental points in Fig. 5 shows the calculated result obtained when adding the spin-wave contributions given by Eq. (6). The only obstacle is that this fit presupposes $k_F \approx 0.22 c^*$, a very small value of the (effective) Fermi wave vector. Such a small value of k_F is, however, consistent with the absence of the similar contribution to the a -axis resistivity, see Fig. 6. Accepting the small value of k_F , only $\mathbf{K} = \pm \mathbf{Q}$ contribute to the sum in Eq. (6), and thus $\mathbf{K} \cdot \hat{\mathbf{u}} = 0$ when $\hat{\mathbf{u}}$ is along the a axis. The calculated result for the a -axis resistivity at ambient pressure is compared with the experimental one in Fig. 6. The dashed line shows the result obtained when neglecting superzone effects, whereas the result shown by the full line includes a minor enhancement due to the superzone energy gaps according to the fitting parameters in Table II. As shown in the insert this enhancement is required for the theory to account for the jump in the resistivity at T_C .

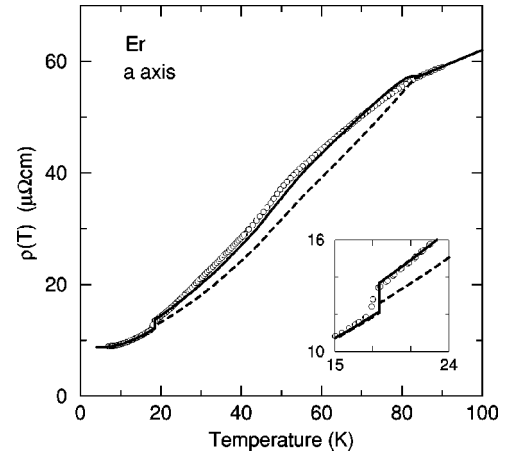


FIG. 6. Experimental and calculated temperature dependence of the a -axis resistivity of Er at ambient pressure. The dashed line shows the calculated result when the superzone effects are neglected.

V. DISCUSSION AND CONCLUSION

The p - T diagram for the magnetic phases in erbium has been derived from measurements of the temperature dependence of the c -axis resistivity at various values of hydrostatic pressure between 0 and 12 kbar. The variation of the Néel temperature with pressure corresponds to $\partial \ln \mathcal{J}(\mathbf{Q}) / \partial \ln V \approx 1.7$, a comparable value to that observed in other heavy rare earths.²⁸ The more rapid reduction of T'_N with pressure indicates that the numerical value of the crystal-field parameter B_2^0 increases by 0.7% per kbar. The strong broadening of the transition between the cycloid and the cone structure, when applying a pressure, makes it difficult to locate the transition precisely. The isothermal behavior of the resistivity at 4.5 K shown in Fig. 2 allows us to place the transition between 1 and 3 kbar, consistent with the theoretical estimate that it should occur at 1.3 kbar at zero temperature.

The unique behavior of the ordering wave vector in Er, that it stays (roughly) constant at large value of the pressure but varies quickly with temperature at ambient pressure, has allowed us to identify the reason for the shortcomings of the Elliott-Wedgwood theory when applied to Er. We conclude that the enhancement factor in the resistivity due to the superzone energy gaps depends on Q . The assumption that the relation between Γ_u and Q is linear, Eq. (9), has then made it possible to explain most of the large differences between the resistivity curves at 1 bar and 7.5 kbar. We may add that in the case of Tm, the remaining discrepancies in the fitting of the superzone effects in the c -axis resistivity, which occur between 30 K and T_N where Q is changing,²⁴ are nearly removed if Γ_c is assumed to depend on Q with a term of the same size as in Eq. (9), but with the opposite sign. The maximum enhancement factors of the resistivity in the two systems are nearly the same, $(1 - \Gamma_c^0)^{-1} \approx 3.5$ in Er (at $p = 7.5$ kbar at zero temperature) and 3.7 in Tm.

The change of Q as a function of temperature is predicted to be another consequence of the superzone energy gaps.^{23,2} Although, in terms of this theory, it is difficult to understand why the temperature variation of Q is much smaller above 6 kbar than it is at ambient pressure. The lock-in energy of the short-period (43)-structure is relatively large, but this is valid

in all cases. Nesting features at the Fermi surface may certainly be important in Er, and they may be strongly influenced by the c/a ratio as suggested by Andrianov (for the case of a helical ordering).²⁹ The c/a ratio changes by 0.5% at T_C without much change in Q . Between T_C and T'_N the c/a ratio decreases 0.2%, from 1.569 to 1.566,² values which are shifted down by approximately 0.2% at a hydrostatic pressure of 10 kbar. These numbers may be interpreted in the way that the modulation of the c -axis moments in Er, but not the helical component, leads to a sensitive change of the superzone effects, and thus also of Q , when the c/a ratio becomes larger than about 1.566. With reference to the c/a -scaling law of Andrianov this signals a transition in the topology of the Fermi surface at a c/a ratio in the neighborhood of 1.575.

If some of the superzone boundaries lie close to a tangential plane of the Fermi surface, the effects of the associated energy gaps will change rapidly with Q . The assumption of a linear dependence of Γ_u on Q made by Eq. (9), is the simplest way of parameterizing a related behavior of the two quantities, but the changes of Γ_u with Q are expected to be more abrupt, with rapid changes of Γ_u whenever a superzone boundary passes through the Fermi surface. This is one possible explanation for the extra anomalies marked by T_a and T_b on the phase diagram in Fig. 3. The transitions between the different commensurate structures may also produce anomalies in the resistivity. Between T'_N and T_C there are many transitions⁴ causing the hysteresis in the temperature dependence of Q . The anomaly marked T_a has also been observed by Watson and Ali in their resistivity study of Er in a b -axis field at ambient pressure.¹² Based on a comparison with the neutron diffraction measurements¹⁰ they propose that it is due to the lock-in transition to the (44) phase. However, neither T_b , and probably nor T_a , in Fig. 3 correlates with the values of Q . This rules out the second explanation, whereas the first one may still survive because of the dependence of the Fermi surface on the volume. A change of the volume may cause the position of the Fermi surface to move, generating the same effect as the opposite change of Q at constant volume. This seems to be the only explanation left for the anomaly at T_b . A dependence of T_b on the volume, or pressure, is consistent with the observation that the anomaly only appears at pressures above a certain threshold value of 4.5 kbar.

The linear extrapolation made in our p - T phase diagram suggests a connection between the anomaly seen at T_a below 4.5 kbar and the reduction of the resistivity occurring at 4.5 K when the pressure is increased from 7.5 to 10.5 kbar. Model calculations indicate that Er, just above T_C , approaches closely the tilted cycloidal phase, where the normal to the cycloidal plane makes a nonzero angle with the basal plane,¹³ and this phase has recently been isolated in the magnetic phase diagram of the Er-Ho alloy system.³⁰ We therefore propose that the anomaly at T_a is due to this transition. This hypothesis needs further experimental investigation. However, it is able to explain the anomaly at T_a without linking it to a certain value of Q , and, partly, the decrease of the resistance between 7.5 and 10.5 kbar at 4.5 K. The solid line in Fig. 2 represents a somewhat speculative interpretation of the isothermal behavior of the c -axis resistivity. The transition between the cone and the tilted cycloid is assumed

to occur at the estimated value of 1.3 kbar, followed immediately by a linear change of Q from $\frac{1}{4} c^*$ to $\frac{2}{7} c^*$ at 3 kbar. Q is then considered to stay constant. The transition between the tilted and nontilted cycloidal phase assumed to occur at 9 kbar should be a second-order one. The precise location is difficult to imitate by the model, instead we have estimated the size of the effect by clamping the cycloidal plane to the a - c plane above 9 kbar.

The last point to discuss is the strong rise of the c -axis resistivity in the cone phase at ambient pressure. This is not reproduced in the model calculations when using the mean-field expression for the absorptive susceptibility, Eq. (5). The variation is accounted for by the spin-wave susceptibility, Eq. (6), but this requires a very small effective Fermi wave vector, $k_F \approx Q$. The application of a c -axis field of at least 2.7 T quenches the c -axis modulated phase, and as shown in Fig. 4, the rapid increase of the resistivity continues up to temperatures of the order of 40 K, far above the regime where the spin-wave expression is valid. Most spin waves and some of the higher lying crystal-field levels are thermally excited at 40 K, making the mean-field susceptibility much more trustworthy than the spin-wave expression at this temperature. The mean-field model accounts accurately for the a -axis resistivity in the cone phase, hence this enhancement seems to be restricted to the c -axis resistivity in the presence of a ferromagnetic component of the c -axis moments. The mean-field model describes the zero-field properties of Er in an acceptable way, but deficiencies appear at nonzero fields.⁴ The two-ion interactions in Er are complex, and it is argued in Ref. 4 that additional two-ion axial anisotropy terms must be present. The two-ion anisotropy terms, which are most likely mediated by the conduction electrons, may contribute directly to the resistivity in the same way as the RKKY coupling, and may be the terms that are responsible for the extra enhancement of the c -axis resistivity.

Complementary neutron-diffraction studies of the low-temperature part of the phase diagram would be valuable. The identification of the tilted cycloidal phase is a challenging problem, as this structure is difficult to detect in diffraction measurements unless a single domain is isolated, which by itself is a nontrivial requirement in the case Er. The present analysis predicts that the lock-in of Q to $\frac{2}{7} c^*$ extends over most of the cycloidal phase not only at 11.5 and 14 kbar but already at a pressure of 6.5 kbar. A direct verification of this behavior by diffraction measurements is desirable. First-principle band-structure calculations of the strong reduction of the Fermi surface area due to the superzone energy gaps induced by the modulated moments in Er or in Tm, and its dependence on the positions of the superzone boundaries, are most desirable.

ACKNOWLEDGMENTS

We are grateful to the UK Engineering and Physical Sciences Research Council, the Danish Natural Science Research Council, and the Austrian Science Foundation (FWF project 12899) for financial support. In addition one of us (M.E.) wishes to acknowledge the Royal Society for a travel grant, and The Austrian Academy of Sciences for acting as host.

- ¹J. W. Cable, E. O. Wollan, W. C. Koehler, and M. K. Wilkinson, *Phys. Rev.* **140**, A1896 (1964).
- ²M. Habenschuss, C. Stassis, S. K. Sinha, H. W. Deckman, and F. H. Spedding, *Phys. Rev. B* **10**, 1020 (1974).
- ³D. Gibbs, J. Bohr, J. D. Axe, D. E. Moncton, and K. L. D'Amico, *Phys. Rev. B* **34**, 8182 (1986).
- ⁴R. A. Cowley and J. Jensen, *J. Phys.: Condens. Matter* **4**, 9673 (1992).
- ⁵J. Jensen and R. A. Cowley, *Europhys. Lett.* **21**, 705 (1993).
- ⁶H. Lin, M. F. Collins, T. M. Holden, and W. Wei, *Phys. Rev. B* **45**, 12 873 (1992).
- ⁷D. F. McMorrow, D. A. Jehan, R. A. Cowley, R. S. Eccleston, and G. J. McIntyre, *J. Phys.: Condens. Matter* **4**, 8599 (1992).
- ⁸R. S. Eccleston and S. B. Palmer, *J. Magn. Magn. Mater.* **104-107**, 1529 (1992).
- ⁹S. W. Zochowski and K. A. McEwen, *J. Magn. Magn. Mater.* **140-144**, 1127 (1995).
- ¹⁰D. A. Jehan, D. F. McMorrow, J. A. Simpson, R. A. Cowley, P. Swadling, and K. A. Clausen, *Phys. Rev. B* **50**, 3085 (1994).
- ¹¹J. J. Rhyne and S. Legvold, *Phys. Rev.* **140**, A2143 (1965).
- ¹²B. Watson and N. Ali, *J. Phys.: Condens. Matter* **8**, 1796 (1996).
- ¹³J. Jensen and A. R. Mackintosh, *Rare Earth Magnetism: Structures and Excitations* (Clarendon Press, Oxford, 1991).
- ¹⁴S. Kawano, B. Lebech, and N. Achiwa, *J. Phys.: Condens. Matter* **5**, 1535 (1993).
- ¹⁵S. Kawano, S. Aa. Sørensen, B. Lebech, and N. Achiwa, *J. Magn. Magn. Mater.* **140-144**, 763 (1995).
- ¹⁶J. E. Milton and T. A. Scott, *Phys. Rev.* **160**, 387 (1967).
- ¹⁷L. I. Vinokurova and E. I. Kondorskii, *Zh. Éksp. Teor. Fiz.* **46**, 1149 (1964) [*Sov. Phys. JETP* **19**, 777 (1964)].
- ¹⁸T. Okamoto, H. Fujii, T. Ito, and E. Tatsumoto, *J. Phys. Soc. Jpn.* **25**, 1729 (1968).
- ¹⁹R. W. Green, S. Legvold, and F. H. Spedding, *Phys. Rev.* **122**, 827 (1961).
- ²⁰A. R. Mackintosh, *Phys. Rev. Lett.* **9**, 90 (1962).
- ²¹H. Miwa, *Prog. Theor. Phys.* **28**, 208 (1962).
- ²²R. J. Elliott and F. A. Wedgwood, *Proc. Phys. Soc. London* **81**, 846 (1963).
- ²³R. J. Elliott and F. A. Wedgwood, *Proc. Phys. Soc. London* **84**, 63 (1964).
- ²⁴M. Ellerby, K. A. McEwen, and J. Jensen, *Phys. Rev. B* **57**, 8416 (1998).
- ²⁵K. A. McEwen and P. Touborg, *J. Phys. F: Met. Phys.* **3**, 1903 (1973).
- ²⁶N. Hessel Andersen, J. Jensen, H. Smith, O. Splitteroff, and O. Vogt, *Phys. Rev. B* **21**, 189 (1979).
- ²⁷M. Atoji, *Solid State Commun.* **14**, 1047 (1974).
- ²⁸*Advances in High Pressure Research*, edited by R. S. Bradley (Academic, New York, 1969), Vol. 3.
- ²⁹A. V. Andrianov, *Pis'ma Zh. Éksp. Teor. Fiz.* **55**, 639 (1992) [*JETP Lett.* **55**, 666 (1992)]; *J. Magn. Magn. Mater.* **140-144**, 767 (1995).
- ³⁰R. A. Cowley, J. A. Simpson, C. Bryn-Jacobsen, R. C. C. Ward, M. R. Wells, and D. F. McMorrow, *Phys. Rev. B* **57**, 8394 (1998).